Article



# Solution-Based Deposition of Anatase Nanoparticle Films for the Mechanical Reinforcement of Steel

Matheus Wilges and Marco Cordeiro *

Posted Date: 30 June 2025

doi: 10.20944/preprints202506.2405.v1

Keywords: Titanium Dioxide; Nanocrystalline Coating; Surface Hardening; Dip-Coating; Nanoindentation; Stainless Steel; Anatase

 doi:10.20944/preprints202506.2405.v1



*Article*

# Solution-Based Deposition of Anatase Nanoparticle Films for the Mechanical Reinforcement of Steel

**Matheus B. Wilges [1] and Marco A. L. Cordeiro [2,*]**

[1] Graduate Program in Materials Science and Engineering, Federal University of São Carlos, Rod. Washington Luis, s/n, São Carlos 13565-905, Brazil

[2] Department of Materials Engineering, Federal University of São Carlos, Rod. Washington Luis, s/n, São Carlos 13565-905, Brazil

* Correspondence: mcordeiro@ufscar.br

**Abstract**

The limited surface hardness of austenitic stainless steels such as SAE 304 often curtails their utility in applications requiring high mechanical durability. To address this, we report on a simple, low-temperature, solution-based method to significantly enhance the surface properties of this steel. Nanocrystalline titanium dioxide ($TiO_2$) films were deposited on SAE 304 substrates via dip-coating from a colloidal suspension of oleate-capped anatase nanoparticles, followed by a non-thermal consolidation process. X-ray diffraction analysis of the resulting film confirmed the formation of a phase-pure anatase coating with an average crystallite size of 5.6 nm, demonstrating the preservation of the nanostructure. Instrumented nanoindentation tests revealed a transformative improvement in mechanical performance; the surface hardness increased by over 200%, from 2.8 GPa for the uncoated substrate to 8.5 GPa for the coated sample. These findings validate that a scalable, non-vacuum, low-temperature deposition route can produce mechanically robust ceramic coatings, presenting an economically attractive and effective pathway for the advanced surface engineering of metallic components.

## 1. Introduction

The engineering of functional surfaces on technologically critical alloys, such as austenitic stainless steels, remains a central theme in materials science.1 While materials like SAE 304 steel are foundational in numerous industries due to their processability and corrosion resistance, their inherent limitations in surface hardness and wear resistance preclude their use in more demanding mechanical applications [1]. A leading strategy to overcome these limitations is the application of nanostructured ceramic coatings [2]. By reducing grain sizes to the sub-100 nm regime, it is possible to leverage phenomena like the Hall-Petch effect to achieve significant improvements in hardness and strength [3,4]. Among the candidate materials, titanium Dioxide (TiO2) is of great interest, valued for its high hardness, exceptional chemical stability, and biocompatibility [4]. Of its primary polymorphs, the anatase crystalline phase is particularly noteworthy, as its formation at the nanoscale is crucial not only for its well-known photocatalytic properties but also for achieving superior mechanical performance in thin films [5].

Most of the protocols to deposit such coatings can be broadly categorized into vapor-phase and liquid-phase routes. Vapor-phase techniques, such as Physical Vapor Deposition (PVD) and Chemical Vapor Deposition (CVD), represent mature and well-understood technologies renowned for producing high-purity, dense films with excellent adhesion [6–8]. However, these methods are fundamentally constrained by their reliance on vacuum conditions, line-of-sight deposition, and often substantial thermal budgets. These factors not only increase capital and operational costs but also limit substrate compatibility and geometric complexity, posing significant challenges to scalability and the coating of large-area components [6].

Liquid-phase deposition offers a compelling alternative, circumventing the need for vacuum and high temperatures. Techniques such as dip-coating are particularly attractive due to their

 doi:10.20944/preprints202506.2405.v1



simplicity, low cost, and ability to coat complex geometries [9]. In this process, film formation is governed by a complex interplay of forces during the substrate withdrawal stage, including viscous drag, gravity, surface tension, and capillarity, with the resulting film thickness being dependent on the withdrawal velocity and the rheological properties of the suspension [10,11]. A critical stage is the solvent evaporation, which drives the nanoparticles into a closely packed assembly. However, this process simultaneously induces significant tensile stresses within the drying film. If these stresses exceed the cohesive strength of the nascent film, they can lead to catastrophic failure through cracking and delamination, often limiting the practical film thickness to a critical value.

A further, more fundamental challenge arises from the nanoparticles themselves. To achieve a stable, monodisperse colloidal suspension, the nanoparticles must be functionalized with surface ligands—in this case, oleate groups —which provide steric repulsion to prevent agglomeration. While essential for the deposition process, this organic layer acts as a physical barrier, inhibiting the inter-particle mass transport required for consolidation into a dense, mechanically coherent ceramic film [12]. The conventional method for removing these ligands is thermal decomposition. However, the high temperatures required for this process inevitably lead to rapid grain growth and coarsening, destroying the initial nano-scale structure and forfeiting the very properties being pursued. This presents a significant processing dilemma: how to effectively consolidate a packed nanoparticle assembly into a dense nanoceramic film without resorting to high-temperature treatments that compromise its nanostructure.

In this study, therefore, addresses this challenge by employing a post-deposition treatment strategy following the dip-coating of a $TiO_2$ nanoparticle suspension onto SAE 304 steel. The objective is to form a mechanically robust, nanocrystalline titania film while preserving its nanoscale features. The investigation validates the success of this approach through structural and mechanical characterization. We confirm the crystallinity of the final consolidated film using X-ray Diffraction (XRD), and provide a quantitative assessment of the enhancement in surface hardness and elastic modulus via instrumented nanoindentation. By demonstrating a significant improvement in mechanical properties, this work validates the potential of a simple, scalable processing route for advanced surface engineering.

## 2. Materials and Methods

### *2.1. Synthesis of Oleate-Capped $TiO_2$ Nanocrystals*

The $TiO_2$ nanocrystals were prepared via a solvothermal synthesis route. In a typical synthesis conducted under a low-humidity controlled atmosphere, a 40 mL solution was prepared by adding titanium(IV) butoxide to oleic acid, which served as the solvent and capping agent, to achieve a final precursor concentration of 0.25 M. After the solution was homogenized, the reaction vessel was sealed and transferred to a closed, stirred reactor system for heat treatment at 230 °C for 48 hours. Upon completion of the reaction, the system was allowed to cool to room temperature. The resulting white solid was collected from the suspension by centrifugation, and the powder was subsequently washed twice with acetone. Finally, the purified oleate-capped $TiO_2$ nanocrystals were dispersed in toluene to form a stable colloidal suspension.

### *2.2. Film Deposition and Processing*

Thin films were deposited on plates of SAE 304 stainless steel. Prior to deposition, the substrates underwent a rigorous cleaning procedure, including sequential washing in deionized water, ethanol, and acetone in an ultrasonic bath.

The cleaned substrates were coated using a dip-coating technique, which involved vertical immersion into the $TiO_2$ nanoparticle suspension, a dwell time of 10 seconds, and withdrawal over 10 seconds (approximate velocity of 5 mm/s). Following withdrawal, the coated substrates were dried in a desiccator. To transform the deposited layer into a solid ceramic film, the dried samples

 doi:10.20944/preprints202506.2405.v1



underwent a final non-thermal post-treatment process designed to remove the organic oleate ligands and promote inter-particle consolidation.

### *2.3. Characterization*

The crystalline structure of the final consolidated film was analyzed by X-ray Diffraction (XRD). Measurements were performed on a Bruker D8 Advance ECO diffractometer using Cu-K$\alpha$ radiation ($\lambda$ = 1.5406 Å). The system was operated at 40 kV and 25 mA, and diffractograms were collected over a 2θ range from 10° to 80°. To visualize the morphology and primary particle size of the synthesized nanocrystals prior to film deposition, Transmission Electron Microscopy (TEM) was employed. The analysis was performed on an FEI Tecnai G² F20 microscope operating at 200 kV.The mechanical properties were evaluated using an Anton Paar MCT3 nanoindenter with a Vickers diamond tip. Load-displacement curves were recorded during indentation cycles to a maximum load of 53 mN on both the uncoated and coated substrates.

## 3. Results

### *3.1. Structural Characterization of the Nanocrystalline Film*

The assessment of the film's phase composition and structural integrity following the deposition and consolidation process was XRD. The diffractogram recorded for the titania film on the SAE 304 steel is presented in Figure 1. The pattern is conspicuously dominated by a set of intense, well-defined diffraction peaks. These sharp reflections, indexed to the (111), (200), and (220) crystallographic planes, are unequivocally assigned to the face-centered cubic (FCC) structure of the austenite phase, which constitutes the bulk of the underlying SAE 304 steel. The high intensity and narrow full width at half-maximum (FWHM) of these peaks are characteristic of the well-crystallized, micrometer-scale grain structure of the metallic substrate, providing a clear structural baseline for the system.

Superimposed upon this strong substrate signal, a distinct, albeit less intense, peak is clearly resolved at a 2θ angle of approximately 25.6°. This peak is unambiguously indexed as the (101) reflection, which is the primary diffraction peak for the anatase polymorph of $TiO_2$. Its presence serves as conclusive evidence of the successful deposition and formation of a crystalline titania film on the steel surface. It is critically important to note the absence of any other $TiO_2$ polymorphs, such as rutile or brookite. The formation of a phase-pure anatase film is a significant outcome, as anatase is a metastable phase that typically transforms to the more thermodynamically stable rutile phase upon thermal treatment at temperatures exceeding 600 °C. The retention of the pure anatase structure indicates that the non-thermal consolidation process employed was effective at creating a crystalline film without inducing deleterious high-temperature phase transformations.

The low relative intensity of the anatase (101) peak is an expected feature, resulting from the very small scattering volume of the ultrathin film compared to the large interaction volume of the bulk substrate sampled by the X-ray beam. More revealing is the pronounced broadening of this peak. This feature is a classic hallmark of materials with crystallite sizes in the nanometer regime. To quantify this, the average crystallite dimension ($D$) was calculated from the FWHM ($\beta$) of the (101) peak using the well-established Scherrer equation: $D = K\lambda/(\beta cos\theta)$, where $K$ is the shape factor (~0.9) and $\lambda$ is the X-ray wavelength. This analysis yielded an average crystallite size of 5.6 nm. This quantitative result confirms that the film is composed of an assembly of nanocrystals, validating that the fundamental nanoscale character of the precursor particles was preserved through the deposition and consolidation process. This crystallite size is well below the critical threshold where the lower surface energy of the anatase phase makes it more thermodynamically stable than rutile, providing a physical basis for the observed phase purity. While the Scherrer formalism does not deconvolve contributions from lattice microstrain, the significant peak broadening strongly suggests that the dominant factor is the nanocrystallite size, a direct consequence of the bottom-up film assembly from discrete nanoparticle precursors.

 doi:10.20944/preprints202506.2405.v1



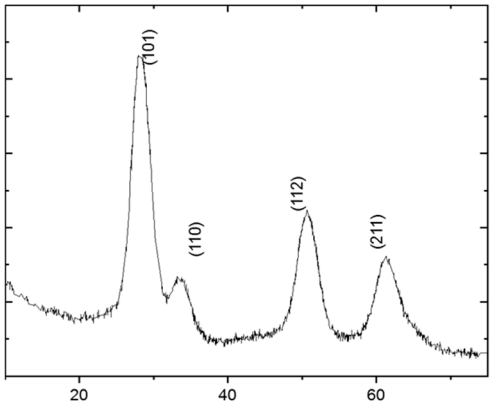


**Figure 1.** X-ray diffractogram of the $TiO_2$ film on the SAE 304 stainless steel substrate. Peaks corresponding to the austenitic steel substrate and the deposited anatase $TiO_2$ phase are indicated.

To provide a direct link between the final film structure and its constituent building blocks, the morphology of the as-synthesized $TiO_2$ nanocrystals was observed using TEM. Figure 2 presents a representative TEM micrograph of these precursor nanoparticles. The image reveals discrete, roughly equiaxed (spherical) nanoparticles with a high degree of size uniformity. Visual inspection of the micrograph shows primary particle sizes consistently in the range of 4-6 nm. This direct observation is in excellent agreement with the average crystallite size of 5.6 nm calculated from the XRD analysis of the final film. This corroboration between techniques confirms that the observed properties of the film are a direct result of its nanoscale constituents and that the consolidation process did not induce significant grain growth. The nanoparticles appear as well-defined, individual crystallites, a critical prerequisite for forming the stable colloidal suspension necessary for depositing a homogeneous film.

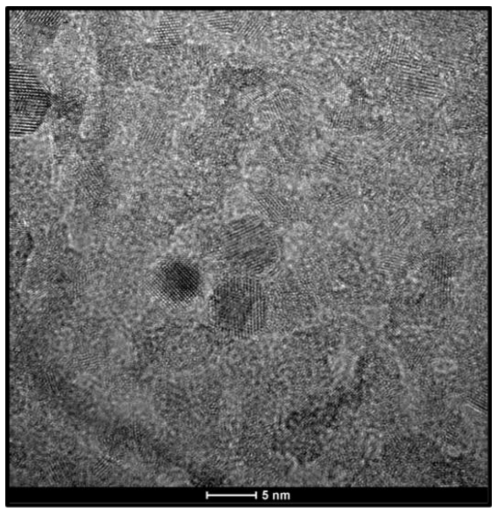


**Figure 2.** Transmission Electron Microscopy (TEM) micrograph of the as-synthesized anatase $TiO_2$ nanoparticles used as the precursor material for film deposition.

*3.2. Quantitative Evaluation of Surface Mechanical Properties*

The functional performance of the nanocrystalline anatase film was evaluated through a quantitative assessment of the surface mechanical properties using instrumented nanoindentation. This technique is the premier method for accurately probing the hardness and elastic modulus of thin films, where conventional micro-scale tests are unsuitable. By precisely measuring the penetration depth ($h$) as a function of applied load ($P$), a detailed map of the material's resistance to plastic and elastic deformation can be generated. The comparative load-displacement ($P - h$) curves for the uncoated SAE 304 substrate and the $TiO_2$-coated sample are presented in Figure 2. The two curves

 doi:10.20944/preprints202506.2405.v1



exhibit markedly different behaviors, providing immediate qualitative evidence of the coating's profound impact. The P-h curve for the bare steel substrate is characteristic of a ductile metal, displaying a large penetration depth for the given maximum load and a substantial residual plastic depth upon unloading. In stark contrast, the curve for the coated sample is significantly shifted to the left, indicating a much higher resistance to initial plastic deformation. Furthermore, the steeper slope of the unloading portion of the curve for the coated sample qualitatively points to a higher elastic modulus, or stiffness.

Quantitatively, for an identical maximum applied load of 53 mN, the indenter penetrated to a final depth of 251 nm in the bare substrate. On the $TiO_2$-coated surface, the same load resulted in a much shallower maximum depth of only 167 nm. This represents a 33% reduction in penetration depth, clearly demonstrating the substantial mechanical reinforcement provided by the ceramic film. For a more detailed analysis, the hardness ($H$) and reduced elastic modulus ($E$) were calculated from the P-h data using the standard Oliver-Pharr method. The results are summarized in Table 1. The analysis reveals a transformative improvement in surface hardness, which increased from 2.8 GPa for the uncoated steel to 8.5 GPa for the $TiO_2$-coated surface—an increase of over 200%. The reduced modulus also showed a notable increase, from 210 GPa for the substrate to 225 GPa for the composite surface.

These measured properties should be interpreted as the effective values of the film-substrate composite system. As the indentation depth of 167 nm is significant relative to the thickness of such films, the mechanical response is inevitably influenced by the more compliant steel substrate. However, the dramatic increase in hardness is unequivocally driven by the ceramic overlayer. A hardness of 8.5 GPa elevates the surface from that of a standard stainless steel to the regime of hard protective coatings. This substantial enhancement is a direct manifestation of the film's dense, nanocrystalline structure. According to the Hall-Petch relationship, the resistance to plastic deformation increases as the grain size decreases. With an exceptionally small crystallite size of 5.6 nm, the film possesses an enormous density of grain boundaries. These boundaries act as effective obstacles to dislocation motion, which is the primary mechanism of plastic deformation. A significantly higher stress is therefore required to initiate and propagate dislocations, resulting in the observed macroscopic increase in hardness. The ability to measure such a high hardness value also implies that the film is dense and possesses strong adhesion to the substrate, as any significant porosity or poor interfacial bonding would have led to film failure, such as cracking or delamination, during the indentation process.

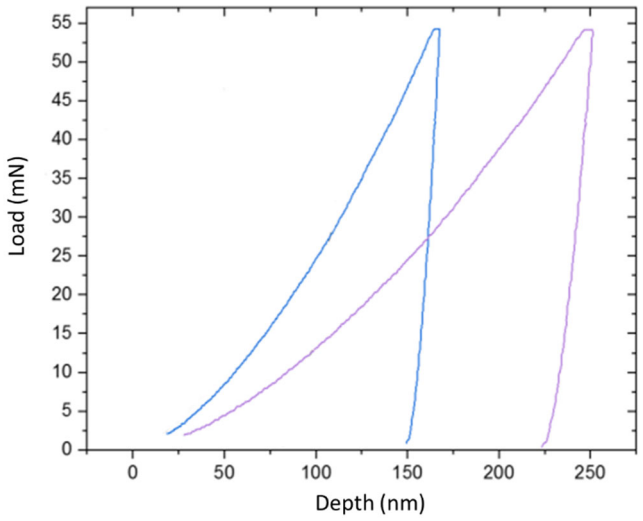


**Figure 2.** Comparative load-displacement curves from nanoindentation tests performed on the uncoated SAE 304 substrate and the $TiO_2$-coated substrate, under a maximum load of 53 mN.

 doi:10.20944/preprints202506.2405.v1



**Table 1.** Summary of mechanical properties obtained from nanoindentation tests on the uncoated and $TiO_2$-coated substrates.

| Sample | Max Depth (nm) | Hardness (H) [GPa] | Reduced Modulus (Er) [GPa] |
|---|---|---|---|
| Uncoated SAE 304 | 251 | 2.8 | 210 |
| $TiO_2$-coated SAE 304 | 167 | 8.5 | 225 |

## 4. Conclusion

This study successfully demonstrated the viability of a simple, solution-based methodology for significantly enhancing the surface mechanical properties of SAE 304 stainless steel. The primary objective was to form a hard, nanocrystalline $TiO_2$ coating using a scalable dip-coating process followed by a non-thermal consolidation step, thereby circumventing the need for complex vacuum systems or high-temperature furnaces that can limit the practicality and applicability of many conventional coating techniques. By leveraging a bottom-up approach starting with pre-synthesized, oleate-capped anatase nanoparticles, we have shown that it is possible to fabricate a functional ceramic film that preserves the critical nanoscale features of its constituent building blocks.

The key findings of this work validate the success of this approach. First, the solvothermal synthesis and subsequent dip-coating process produced a uniform nanoparticle layer on the steel substrate. The subsequent non-thermal treatment was effective in consolidating this layer into a coherent film. Structural characterization by X-ray Diffraction was crucial in confirming the composition and structure of the final coating. The results indicated the formation of a phase-pure anatase $TiO_2$ film, with the complete absence of other polymorphs, such as rutile. Furthermore, the analysis of the XRD peak broadening yielded an average crystallite size of 5.6 nm, confirming that the nanostructure was successfully retained throughout the entire process.

The most significant outcome of this study is the profound improvement in the surface's mechanical performance, which was quantified by instrumented nanoindentation. The nanocrystalline anatase film imparted a dramatic increase in hardness, elevating the value from 2.8 GPa for the uncoated substrate to 8.5 GPa for the coated surface, an improvement of over 200%. This transformation is attributed to the intrinsic hardness of the ceramic and the powerful Hall-Petch strengthening mechanism, where the ultra-high density of grain boundaries in the nanocrystalline film effectively impedes dislocation motion. This work provides important insights into the production of nanoceramics through simple and economically viable protocols.

In a broader context, this research addresses a fundamental challenge in materials processing: the consolidation of ligand-stabilized nanoparticles into a dense, functional material without resorting to high-temperature treatments that destroy their nanoscale advantages. The success of this low-temperature route highlights its potential for coating a wide variety of substrates, including those sensitive to heat. Looking forward, future work should focus on exploring the influence of processing parameters, such as the duration of the post-treatment, on the final film properties. Additionally, evaluating the long-term performance of these coatings, including their wear and corrosion resistance, and extending the deposition methodology to other substrates like glass and polymers would be valuable next steps.

**Acknowledgments:** This study was financed in part by the Coordenação de Aperfeiçoamento de Pessoal de Nível Superior - Brasil (CAPES) - Finance Code 001. The authors gratefully acknowledge the Federal University of São Carlos (UFSCar) and the Graduate Program in Materials Science and Engineering (PPGCEM – UFSCar) for their essential technical infrastructure and scholarly support, which significantly contributed to the successful execution of this study.

 doi:10.20944/preprints202506.2405.v1



## References


1. Rezayat, M.; Karamimoghadam, M.; Moradi, M.; Casalino, G.; Rovira, J. J. R.; Mateo, A., Overview of Surface Modification Strategies for Improving the Properties of Metastable Austenitic Stainless Steels. *Metals* **2023,** *13* (7).
2. Wang, Z. W.; Li, Y.; Zhang, Z. H.; Zhang, S. Z.; Ren, P.; Qiu, J. X.; Wang, W. W.; Bi, Y. J.; He, Y. Y., Friction and wear behavior of duplex-treated AISI 316L steels by rapid plasma nitriding and (CrWAlTiSi)N ceramic coating. *Results in Physics* **2021,** *24*.
3. Armstrong, R. W., 60 Years of Hall-Petch: Past to Present Nano-Scale Connections. *Materials Transactions* **2014,** *55* (1), 2-12.
4. Wang, Y. J.; Zhang, J. Z.; Zhao, Y. S., Strength weakening by nanocrystals in ceramic materials. *Nano Letters* **2007,** *7* (10), 3196-3199.
5. Chen, X.; Mao, S. S., Titanium dioxide nanomaterials: Synthesis, properties, modifications, and applications. *Chemical Reviews* **2007,** *107* (7), 2891-2959.
6. Schalk, N.; Tkadletz, M.; Mitterer, C., Hard coatings for cutting applications: Physical vs. chemical vapor deposition and future challenges for the coatings community. *Surface & Coatings Technology* **2022,** *429*.
7. von Niessen, K.; Gindrat, M.; Refke, A., Vapor Phase Deposition Using Plasma Spray-PVD™. *Journal of Thermal Spray Technology* **2010,** *19* (1-2), 502-509.
8. Santecchia, E.; Hamouda, A. M. S.; Musharavati, F.; Zalnezhad, E.; Cabibbo, M.; Spigarelli, S., Wear resistance investigation of titanium nitride-based coatings. *Ceramics International* **2015,** *41* (9), 10349-10379.
9. Ray, S. C.; Karanjai, M. K.; DasGupta, D., Tin dioxide based transparent semiconducting films deposited by the dip-coating technique. *Surface & Coatings Technology* **1998,** *102* (1-2), 73-80.
10. Chen, Z. X.; Townsend, J.; Aprelev, P.; Gu, Y.; Burtovyy, R.; Luzinov, I.; Kornev, K. G.; Peng, F., Magnetic Submicron Mullite Coatings with Oriented SiC Whiskers. *Acs Applied Materials & Interfaces* **2018,** *10* (14), 11907-11919.
11. Niazmand, M.; Maghsoudipour, A.; Alizadeh, M.; Khakpour, Z.; Kariminejad, A., Effect of dip coating parameters on microstructure and thickness of 8YSZ electrolyte coated on NiO-YSZ by sol-gel process for SOFCs applications. *Ceramics International* **2022,** *48* (11), 16091-16098.
12. Figueira, R. B.; Silva, C. J. R.; Pereira, E. V. Influence of Experimental Parameters Using the Dip-Coating Method on the Barrier Performance of Hybrid Sol-Gel Coatings in Strong Alkaline Environments *Coatings* [Online], 2015, p. 124-141.